CHAPTER 1

LOOPHOLE-FREE TEST OF QUANTUM NONLOCALITY WITH CONTINUOUS VARIABLES OF LIGHT

R. García-Patrón and N. J. Cerf

QUIC, Ecole Polytechnique, CP 165, Université Libre de Bruxelles, 1050 Brussels, Belgium

J. Fiurášek

Department of Optics, Palacký University, 17. listopadu 50, 77200 Olomouc, Czech Republic

It is shown that a loophole-free Bell test can be achieved using continuous variables of light. A feasible optical setup is proposed for this purpose, based on a non-Gaussian state of light and high-efficiency homodyne detectors. The non-Gaussian entangled state can be generated from a two-mode squeezed vacuum state by subtracting a single photon from each mode using beam splitters and standard low-efficiency single-photon detectors. A Bell violation exceeding 1% can be attained with 6 dB squeezed light and an homodyne efficiency around 95%. A detailed feasibility analysis, including the effect of the detector efficiency, the electronic noise, the impurity of the non-Gaussian state, and the probability of false triggers, suggests that this method opens a promising avenue towards a complete experimental Bell test.

1. Introduction

Over the last century, quantum physics has developed into a powerful tool, allowing the description of a wide range of phenomena at the microscopic scale. Technologies such as lasers, NMR, or semi-conductor based systems would be impossible without quantum physics. Even if quantum theory has reached a high level of maturity, some of its basic concepts still are very counterintuitive and have puzzled physicists since the early days of the theory. Feynman's famous expression "I think I can safely say that nobody understands quantum mechanics" is a good illustration of this opinion.

EPR
hidden-variable model
Bell inequalities
local realism

Since the inception of quantum mechanics, several physicists have considered this counterintuitive aspect as an evidence of the incompletude of the theory. There have been repeated suggestions that its probabilistic features may possibly be described by an underlying deterministic substructure. The first attempt in this direction originates from the famous paper by Einstein, Podolsky, and Rosen (EPR) [1] in 1935. There, it was advocated that if "local realism" (causality + deterministic substructure) is taken for granted, then quantum theory is an incomplete description of the physical world.

The EPR argument gained a renewed attention in 1964, when John Bell derived his famous inequalities, which must be satisfied within the framework of any local realistic theory [2]. Bell showed that any such deterministic substructure model (also called "hidden-variables model"), if local, yields predictions that significantly differ from those of quantum mechanics. The merit of Bell inequalities lies in the possibility to test them experimentally, allowing physicists to test whether either quantum mechanics or local realism is the correct description of Nature.

2. Bell inequalities

In this chapter, we will use the Clauser-Horne-Shimony-Holt inequality (called Bell-CHSH inequality in the following), originally devised for a two-qubit system [3]. Let us consider the following thought experiment, which we will analyze from the point of view of local realism. The experiment involves three distant parties, Sophie, Alice, and Bob. Sophie (the source) prepares a bipartite state and distribute it to Alice and Bob (the two usual partners), see Fig. 1. Then, Alice and Bob randomly and independently decide between one of two possible quantum measurements A_1 or A_2 (B_1 or B_2), which should have only two possible outcomes $+1$ or -1. The timing of the experiment should be arranged in such a way that Alice and Bob do their measurements in a causally disconnected manner. Thereby, Alice's measurement cannot influence Bob's, and vice-versa. Local realism implies two assumptions:

(1) Realism: the physical properties A_1, A_2, B_1, B_2 have definite values a_1, a_2, b_1, b_2, which exist independently of their observation. This implies the existence of a probability distribution $P(a_1, a_2, b_1, b_2)$, dependent on how Sophie generates the bipartite state.
(2) Locality: Alice's measurement choice and outcome do not influence the result of Bob's measurement, and vice-versa. The measurement events are separated by a spacelike interval.

CHSH inequalities

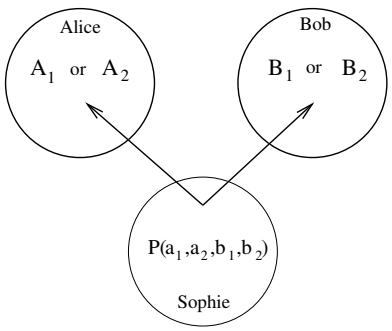

Fig. 1. Sophie prepares a bipartite state and distributes it to Alice and Bob, who perform each a measurement. Alice measures either A_1 or A_2, while Bob measures B_1 or B_2. In a local realistic theory, there must exist an underlying probability distribution $p(a_1, a_2, b_1, b_2)$, generated by Sophie.

If we consider local realism as the correct description of the physical world, then we obtain the Bell-CHSH inequality

$$S = |\langle a_1 b_1\rangle + \langle a_1 b_2\rangle + \langle a_2 b_1\rangle - \langle a_2 b_2\rangle| \leq 2, \tag{1}$$

where $\langle a_j b_k\rangle$ denotes the average over the subset of experimental data where Alice measured a_j and, simultaneously, Bob measured b_k. Indeed, if there is an underlying probability distribution $p(a_1, a_2, b_1, b_2)$, then each realization of it contributes by $a_1(b_1 + b_2) + a_2(b_1 - b_2) = \pm 2$ to the average, implying Eq. (1).

Now, if we consider that Sophie generates and distributes an entangled pair of qubits, quantum mechanics predicts $S = 2\sqrt{2}$, which is in contradiction with local realism. Thus, an experimental test of Bell-CHSH inequalities where a violation of $S \leq 2$ is observed disproves any classical (local realistic) description of Nature.

3. Experimental Bell test and related loopholes

From the beginning of the 80's, many experimental Bell tests [4,5,6,7,8,9,10] have been performed, observing the violation of Bell inequalities predicted by quantum mechanics. All these schemes used optical setups because, at that time, it was the only known way of generating and distributing entangled particles (photons) at a distance in order to make Alice's and Bob's measurements causally disconnected. Unfortunately, the available single-photon detectors suffer from a low efficiency η_{PD}, which can be exploited by a local realistic model to yield a violation. Thus, to reject local realism,

loopholes ! detector-efficiency

loopholes ! locality

it is necessary to make the extra assumption that the registered pairs form a fair sample of the emitted pairs. So, from a logical point of view, these experiments do not succeed in ruling out a local realistic model; this is the so-called *detector-efficiency loophole* [11,12,13]. This loophole has been closed in a recent experiment with trapped ions [14], thanks to the high efficiency of the measurement of the ion states. However, the ions were held in a single trap, only several micrometers apart, so that the measurement events were not spacelike separated, opening in turn the so-called *locality loophole* [15,16].

So far, no experimental test has succeeded to close both loopholes at the same time, that is, the measured correlations may be explained in terms of local realistic theories exploiting the low detector efficiency or the timelike interval between the two detection events. It was suggested that two distant trapped ions can be entangled via entanglement swapping by first preparing an entangled state of an ion and a photon on each side and then projecting the two photons on a maximally entangled singlet state [17,18,19,20]. Very recently, the first step toward this goal, namely the entanglement between a trapped ion and a photon emitted by the ion, has been observed experimentally [21]. However, the entanglement swapping would require interference of two photons emitted by two different ions, which is experimentally very challenging. An interesting alternative to the atom-based approaches [17,22,23] consists of all-optical schemes based on continuous variables of light. Indeed, the balanced homodyne detection used in these schemes can exhibit a high detection efficiency [24], sufficient to close to detection loophole.

4. Bell test with continuous variables of light

Quantum continuous variables of light have been successful used to realize some of the standard informational tasks traditionally based on qubits. Unfortunately, the entangled two-mode squeezed state that can easily be generated experimentally [25,26,27] cannot be directly employed to test Bell inequalities with homodyning. Indeed, as noted by Bell himself, this state is described by a positive-definite Gaussian Wigner function, which thus provides a local realistic model that can explain all correlations between quadrature measurements (carried out by balanced homodyne detectors). Thus, similarly as in the case of the purification of continuous variable entanglement [28,29,30,31,32], one has to go beyond the class of Gaussian states or Gaussian operations.

In particular, it is possible to obtain a Bell violation with a Gaussian two-mode squeezed vacuum state by performing a non-Gaussian measure-

ment, for example a photon-counting measurement [33]. As shown in Fig. 2, Sophie prepares an entangled state and distributes it to Alice and Bob. The two possible measurements on Alice's and Bob's sides consist in randomly choosing between applying the displacement $D(\alpha)$ or no displacement, followed by a measurement of the parity of the number of photons n impinging on the single-photon detector. The resulting parity $a_i = (-1)^n$ gives the binary result used in the Bell-CHSH inequality. It can be shown[33] that

Wigner function

$$S = |W(0,0) + W(\alpha,0) + W(0,\alpha) - W(\alpha,\alpha)| \tag{2}$$

where $W(x,p)$ is the Wigner function of the entangled state, violates the Bell-CHSH inequality $S \leq 2$ by about 10% for an appropriate choice of α. Recent proposals using more abstract measurements described in Refs. [34,35,36] gave similar results. Note, however, that these measurements are either experimentally infeasible or suffer from a very low detection efficiency, thereby re-opening the detection loophole.

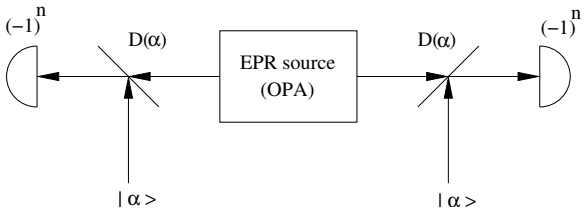

Fig. 2. Bell test using the parity of the number of photons impinging on each photodetector. Sophie prepares an entangled state (EPR) and distributes it to Alice and Bob. Each of them either applies a displacement $D(\alpha)$ or not, and uses the parity of the number of photon measured using a photodetectors with single-photon resolution [33].

Considering the current state of the art in quantum optics technologies, the scheme based on high-efficiency homodyne detection seems to be the most promising way of closing the detection loophole. However, since homodyning is a Gaussian measurement, it is then necessary to generate highly non-classical non-Gaussian entangled states, whose Wigner function is not positive definite. In addition, one has to develop a method for converting the continuous result obtained by homodyne measurement into a binary result (the so-called "binning" method).

Several recent theoretical works have demonstrated that a violation of Bell inequalities can be observed using balanced homodyning provided that specific entangled light states such as pair-coherent states, squeezed

Schrödinger cat-like states, or specifically tailored finite superpositions of Fock states, are available [37,38,39,40]. More specifically, the violation of the Bell-CHSH inequality was derived in Ref. [39] for a state of the form

$$|\psi_{\rm in}\rangle_{AB} = \sum_{n=0}^{\infty} c_n |n,n\rangle_{AB}, \tag{3}$$

with $|n\rangle$ denoting Fock states, and a binning based on the sign of the measured quadrature. Optimizing over the quadrature angles and probability amplitudes c_n (see Fig. 3), one obtains a maximal Bell-CHSH inequality violation of $S = 2.076$. Interestingly, it was shown in Ref. [40] that the highest possible violation of $S = 2\sqrt{2}$ can be obtained with the bipartite state

$$|\psi_{\rm in}\rangle_{AB} = |f,f\rangle + e^{i\theta}|g,g\rangle, \tag{4}$$

where $f(q)$ and $g(q)$ are the wave functions of some specific states, and a more complicated binning based on the roots of $f(q)$ and $g(q)$ is used. Unfortunately, no feasible experimental scheme is known today that could generate the states required in Refs. [37,38,39,40].

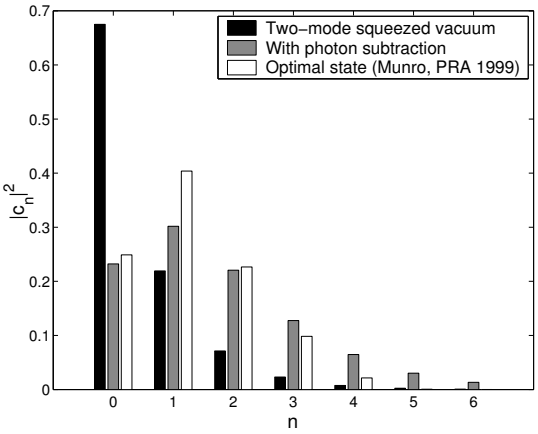

Fig. 3. Probabilities $|c_n|^2$ in the Fock basis of the two-mode squeezed vacuum state with $\lambda = 0.57$ (black), the non-Gaussian state obtained from the previous state by subtracting one photon from each mode (grey), and the optimal state of Ref. [39] (white).

Recently, it was shown by us together with J. Wenger, R. Tualle-Brouri and P. Grangier [41], and independently by Nha and Carmichael [42], that a very simple non-Gaussian state obtained by subtracting a single photon

from each mode of a two-mode squeezed vacuum state can exhibit a Bell violation with homodyning. Note that this non-Gaussian state is close to the optimal state obtained in Ref. [39], as is visible in Fig. 3, and gives a violation of $S = 2.046$.

de-gaussification
homodyne detection
optical parametric amplifier (OPA)
photon subtraction

An essential feature of this proposal is that the photon subtraction can be successfully performed with low-efficiency single-photon detectors [43,44,45], which renders the setup experimentally feasible. In fact, the basic building block of the scheme, namely the de-gaussification of a single-mode squeezed vacuum via single-photon subtraction, has recently been demonstrated experimentally [46].

5. Loophole-free Bell test using homodyne detectors

The conceptual scheme of the proposed experimental setup is depicted in Fig. 4. A source generates a two-mode squeezed vacuum state in modes A and B. This can be accomplished, e.g., by means of non-degenerate optical parametric amplification in a $\chi^{(2)}$ nonlinear medium or by generating two single-mode squeezed vacuum states and combining them on a balanced beam splitter. Subsequently, the state is de-gaussified by conditionally subtracting a single photon from each beam. A tiny part of each beam is reflected from a beam splitter BS_A (BS_B) with a high transmittance T. The reflected portions of the beams impinge on single-photon detectors such as avalanche photodiodes. A successful photon subtraction is heralded by a click of each photodetector PD_A and PD_B [45].

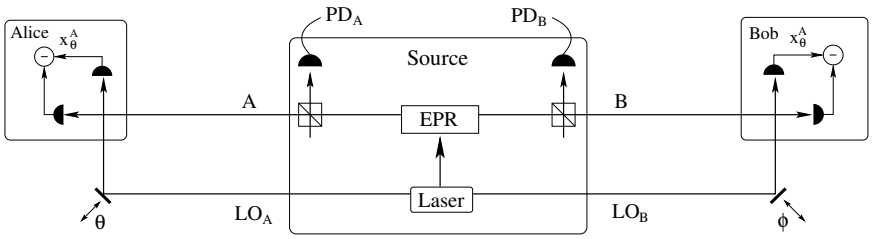

Fig. 4. Proposed experimental setup for performing a Bell test with balanced homodyning. The source emits a two-mode squeezed vacuum state in modes A and B. A small part of the beams is diverted by two highly unbalanced beam splitters BS_A and BS_B, and sent to the single-photon detectors PD_A and PD_B. The two remaining beams A and B, which are conditionally prepared in a non-Gaussian entangled state, are sent to Alice and Bob, who perform each a balanced homodyne detection using their local oscillator LO_A and LO_B.

event-ready detectors

In practice, the available photodetectors exhibit a single-photon sensitivity but not a single-photon resolution, that is, they can distinguish the absence and presence of photons but cannot measure the number of photons in the mode. Nevertheless, this is not a problem here because in the limit of high T, the most probable event leading to the click of a photodetector is precisely that a single photon has been reflected by the beam splitter. The probability of an event where two or more photons are subtracted from a single mode is smaller by a factor of $\approx 1-T$ and becomes totally negligible in the limit of $T \to 1$. Another important feature of the scheme is that the detector efficiency $\eta_{\rm PD}$ can be quite low because a small $\eta_{\rm PD}$ only reduces the success rate of the conditional single-photon subtraction, but does not significantly decrease the fidelity of this operation.

After generation of the non-Gaussian state, the beams A and B together with the appropriate local oscillators LO_A and LO_B are sent to Alice and Bob, who then randomly and independently measure one of two quadratures $x^A_{\theta_j}$, $x^B_{\phi_k}$ characterized by the relative phases θ_1, θ_2 and ϕ_1, ϕ_2 between the measured beam and the corresponding local oscillator.

To avoid the locality loophole, the whole experiment has to be carried out in the pulsed regime and a proper timing is necessary. In particular, the measurement events on Alice's and Bob's sides (including the choice of phases) have to be spacelike separated. A specific feature of the proposed setup is that the non-Gaussian entangled state is conditionally generated when both "event-ready" (see [15] p. 29 and 105) detectors PD_A and PD_B click. This can be viewed as some preselection of the non-Gaussian state at the source. However, we would like to stress that this does not open any causality loophole if proper timing is satisfied. Namely, in each experimental run, the detection of the clicks (or no-clicks) of photodetectors PD_A and PD_B at the source should be spacelike separated from Alice's and Bob's measurements. This guarantees that the choice of the measurement on Alice's and Bob's sides cannot in any way influence the conditioning "event-ready" measurement [15,17,41].

In the proposed experiment, Alice and Bob measure quadratures which have a continuous spectrum. These quadratures can be discretized by postulating that the outcome is $+1$ when $x \geq 0$ and -1 otherwise. The two different measurements on each side correspond to the choices of two relative phases θ_1, θ_2 and ϕ_1, ϕ_2. Thus, the quantum correlation $E(\theta_j, \phi_k) \equiv \langle a_j b_k \rangle$ can be expressed as

$$E(\theta_j, \phi_k) = \int_{-\infty}^{\infty} \mathrm{sign}(x^A_{\theta_j} x^B_{\phi_k}) P(x^A_{\theta_j}, x^B_{\phi_k}) dx^A_{\theta_j} dx^B_{\phi_k}, \qquad (5)$$

where $P(x^A_{\theta_j}, x^B_{\phi_k}) \equiv \langle x^A_{\theta_j}, x^B_{\phi_k} | \rho_{\text{out},AB} | x^A_{\theta_j}, x^B_{\phi_k} \rangle$ is the joint probability distribution of the two commuting quadratures $x^A_{\theta_j}$ and $x^B_{\phi_k}$, and $\rho_{\text{out},AB}$ denotes the (normalized) conditionally generated non-Gaussian state of modes A and B. The entire data analysis must be performed on a pulsed basis, with Sophie sending time-tagged light pulses (local oscillator and squeezed light) to Alice and Bob. In each experimental run, Sophie records whether her two photodetectors PD_A and PD_B clicked, while Alice and Bob carry out space-like separated measurements of one of two randomly chosen quadratures. After registering a large number of events, the three partners discard all events obtained in measurement runs where either PD_A or PD_B did not click. The correlation coefficients $\langle a_j b_k \rangle$ are then evaluated from all remaining events, and plugged into the S parameter (1).

non-Gaussian state

6. Simplified model with ideal photodetectors

First, we consider a simplified description of the setup, assuming ideal photodetectors ($\eta_{\text{PD}} = 1$) with single-photon resolution and conditioning on detecting exactly one single photon at each detector [43,44]. This idealized treatment is valuable since it provides an upper bound on the practically achievable Bell factor S. Moreover, as noted above, in the limit of high transmittance $T \to 1$, a realistic (inefficient) detector with single-photon sensitivity is practically equivalent to this idealized detector.

The two-mode squeezed vacuum state is expressed in the Fock basis as

$$|\psi_{\text{in}}(\lambda)\rangle_{AB} = \sqrt{1-\lambda^2} \sum_{n=0}^{\infty} \lambda^n |n,n\rangle_{AB}, \tag{6}$$

where $\lambda = \tanh(s)$ and s is the squeezing constant. In the case of ideal photodetectors, the single-photon subtraction results in the state

$$|\psi_{\text{out}}\rangle_{AB} \propto \hat{a}_A \hat{a}_B |\psi_{\text{in}}(T\lambda)\rangle_{AB}, \tag{7}$$

where $\hat{a}_{A,B}$ are annihilation operators and the parameter λ is replaced by $T\lambda$ in order to take into account the transmittance of BS_A and BS_B. A detailed calculation shows that this non-Gaussian state has the form

$$|\psi_{\text{out}}\rangle_{AB} = \sqrt{\frac{(1-T^2\lambda^2)^3}{1+T^2\lambda^2}} \sum_{n=0}^{\infty} (n+1)(T\lambda)^n |n,n\rangle_{AB}, \tag{8}$$

For pure states exhibiting perfect photon-number correlations such as Eq. (8), the correlation coefficient (5) depends only on the sum of the angles, $E(\theta_j, \phi_k) = \mathcal{E}(\theta_j + \phi_k)$. With the help of the general formula derived

Bell factor

in Ref. [39], we obtain for the state (8)

$$\mathcal{E}(\varphi) = \frac{(1-T^2\lambda^2)^3}{1+T^2\lambda^2} \sum_{n>m} \frac{8\pi(2T\lambda)^{n+m}}{n!m!(n-m)^2}(n+1)(m+1) \times[\mathcal{F}(n,m)-\mathcal{F}(m,n)]^2 \cos[(n-m)\varphi], \quad (9)$$

where $\mathcal{F}(n,m) = \Gamma^{-1}((1-n)/2)\Gamma^{-1}(-m/2)$ and $\Gamma(x)$ stands for the Euler gamma function.

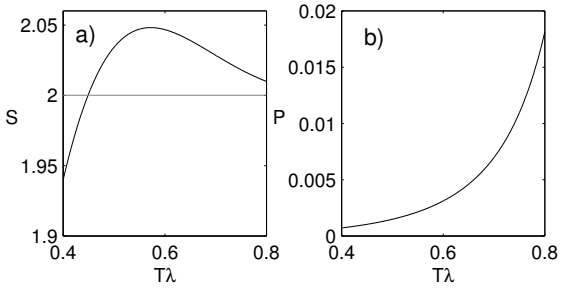

Fig. 5. (a) Bell factor S as a function of the effective squeezing parameter $T\lambda$ for $\theta_1 = 0$, $\theta_2 = \pi/2$, $\phi_1 = -\pi/4$ and $\phi_2 = \pi/4$. (b) Probability P of successful conditional generation of the state $|\psi_{\rm out}\rangle$ as a function of the effective squeezing parameter $T\lambda$, assuming $T = 0.95$.

We have numerically optimized the angles $\theta_{1,2}$ and $\phi_{1,2}$ to maximize the Bell factor S. It turns out that, for any λ, it is optimal to choose $\theta_1 = 0, \theta_2 = \pi/2$, $\phi_1 = -\pi/4$ and $\phi_2 = \pi/4$. The Bell factor S for this optimal choice of angles is plotted as a function of the effective squeezing parameter $T\lambda$ in Fig. 5(a), and the corresponding probability of success of the conditional preparation of the state $|\psi_{\rm out}\rangle$ is plotted in Fig. 5(b). We can see that S is higher than 2 so the Bell-CHSH inequality is violated when $T\lambda > 0.45$. The maximal violation is achieved for $T\lambda \approx 0.57$, giving $S \approx 2.048$. This violation is quite close to the maximum Bell factor $S = 2.076$ that can be reached with homodyne detection, sign binning, and arbitrary states exhibiting perfect photon-number correlations $|\psi\rangle = \sum_n c_n|n,n\rangle$ [39].

7. Realistic model

Here, we consider a realistic scheme with inefficient ($\eta_{\rm PD} < 1$) photodetectors exhibiting single-photon sensitivity but no single-photon resolution,

and realistic balanced homodyning with efficiency $\eta_{\rm BHD} < 1$. The mathematical description of this realistic model is simplified by working in the phase-space representation and using the Wigner function formalism. Even though the state used for the Bell test is intrinsically non-Gaussian, it can be expressed as a linear combination of Gaussian states, so all the powerful Gaussian tools may still be used [47].

Wigner function

7.1. *Calculation of the Wigner function*

As shown in Fig. 6, the modes A and B are initially prepared in a two-mode squeezed vacuum state associated with the Wigner function

$$W_{AB}(r) = W_G(r_{AB};\Gamma_{\rm in}) = \frac{\sqrt{\det\Gamma_{\rm in}}}{\pi^2} e^{-r_{AB}^T \Gamma_{\rm in} r_{AB}}, \qquad (10)$$

where W_G means Gaussian Wigner function, $r_{AB} = (x_A, p_A, x_B, p_B)^T$, and $\Gamma_{\rm in}$ is the inverse of the covariance matrix of a two-mode squeezed vacuum state.

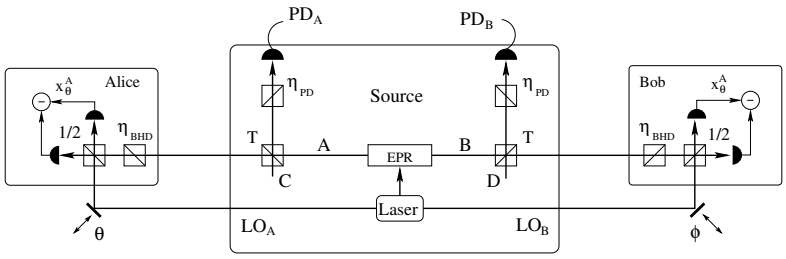

Fig. 6. Detailed optical setup of the proposed Bell test taking into account the realistic single-photon ($\eta_{\rm PD} < 1$) and homodyne ($\eta_{\rm BHD} < 1$) detectors.

The output state $\rho_{{\rm out},AB}$ is prepared by conditioning on observing clicks at both photodetectors PD_A and PD_B. These detectors respond with two different outcomes, either a click, or no click. Mathematically, an ideal detector with single-photon sensitivity is described by a two-component positive operator valued measure (POVM) consisting of projectors onto the vacuum state and the rest of the Hilbert space, $\Pi_0 = |0\rangle\langle 0|$ and $\Pi_1 = I - |0\rangle\langle 0|$. The resulting conditionally prepared state $\rho_{{\rm out},AB}$ is thus

$$\rho_{{\rm out},AB} = {\rm Tr}_{CD}[\mathcal{M}(\rho_{ABCD} \otimes |0\rangle_{C,D}\langle 0|)(I_{AB} \otimes \Pi_{1,C} \otimes \Pi_{1,D})]. \qquad (11)$$

where $\mathcal{M}$ denotes the Gaussian CP map that describes the mixing of modes A with C (and B with D) on the unbalanced beam splitters BS_A (and BS_B),

Bell factor

followed by the "virtual" lossy channels of transmittance $\eta_{\rm PD}$ (and $\eta_{\rm BHD}$) modeling the inefficiency of the single-photon detectors (and homodyne detectors). As a result, the Wigner function of the state $\rho_{{\rm out},AB}$ can be written as a linear combination of 4 Gaussian functions,

$$W_{{\rm out},AB}(r) = \frac{1}{P_G}\sum_{j=1}^{4} C_j W_G(r;\Gamma_j). \tag{12}$$

where P_G is the probability of successful photon subtractions. The correlation matrices Γ_j and the coefficients C_j can be expressed in terms of $\Gamma_{\rm in}$, see [47] for a detailed derivation.

7.2. *Resulting Bell violation*

The joint probability distribution $P(x^A_{\theta_j}, x^B_{\phi_k})$ of the quadratures $x^A_{\theta_j}$ and $x^B_{\phi_k}$ appearing in Eq. (5) for the correlation coefficient $E(\theta_j,\phi_k)$ can be obtained from the Wigner function (12) as a marginal distribution:

$$P(x^A_{\theta_j}, x^B_{\phi_k}) = \int_{-\infty}^{\infty}\int_{-\infty}^{\infty} W_{{\rm out},AB}(S_{\rm sh}^T r_{\theta_j,\phi_k})\, dp^A_{\theta_j}\, dp^B_{\phi_k}, \tag{13}$$

where $r_{\theta_j,\phi_k} = [x^A_{\theta_j}, p^A_{\theta_j}, x^B_{\phi_k}, p^B_{\phi_k}]$ and the symplectic matrix $S_{\rm sh}$ describes local phase shifts that must be applied to modes A and B in order to map the measured quadratures $x^A_{\theta_j}$ and $x^B_{\phi_k}$ onto the quadratures x^A and x^B, respectively. As can be seen in Fig. 7(a,b), the joint probability P exhibits two peaks, both located in a quadrant where Alice's and Bob's measured quadratures have the same sign. This double-peak structure is a clear signature of the non-Gaussian character of the state. The plots for the corresponding Gaussian state (before photon subtraction) are also shown in Fig. 7(c,d) for comparison.

The Bell factor can be expressed as

$$S = E(\theta_1,\phi_1) + E(\theta_1,\phi_2) + E(\theta_2,\phi_1) - E(\theta_2,\phi_2) \tag{14}$$

where, taking into account the sign binning, the normalization of the joint probability distribution $P(x^A_{\theta_j}, x^B_{\phi_k})$, and its symmetry $P(x^A_{\theta_j}, x^B_{\phi_k}) = P(-x^A_{\theta_j}, -x^B_{\phi_k})$, we can express the correlation coefficient as

$$E(\theta_j,\phi_k) = 4\int_0^{\infty}\int_0^{\infty} P(x^A_{\theta_j}, x^B_{\phi_k})\, dx^A_{\theta_j}\, dx^B_{\phi_k} - 1. \tag{15}$$

This last integral can be easily evaluated analytically [47].

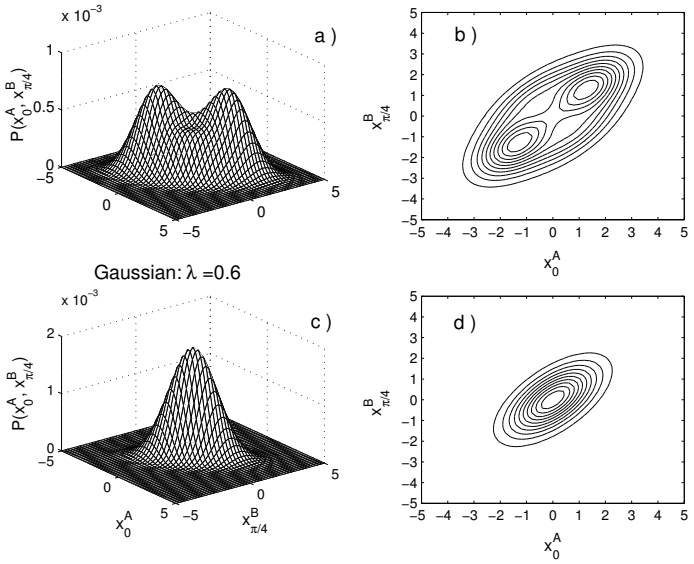

Fig. 7. Joint probability distribution $P(x^A_{\theta_j}, x^B_{\phi_k})$. Panels (a) and (b) show the distribution for the conditionally-prepared non-Gaussian state with $T = 0.99$. Panels (c) and (d) correspond to the initial Gaussian two-mode squeezed vacuum state. The curves are plotted for perfect detectors $\eta_{\rm PD} = \eta_{\rm BHD} = 100\%$, squeezing $\lambda = 0.6$ and $\theta_{\rm Alice} = 0$ and $\phi_{\rm Bob} = \pi/4$.

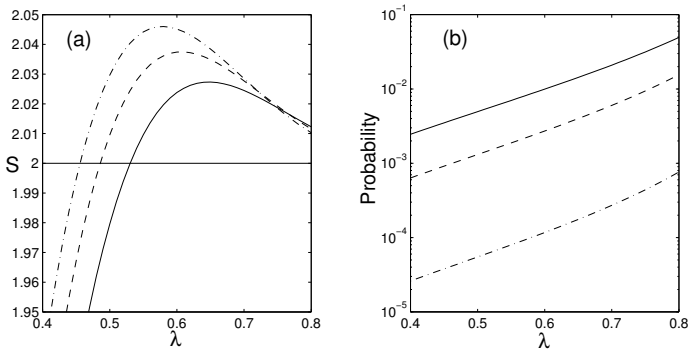

Fig. 8. Violation of the Bell-CHSH inequality with the conditionally-prepared non-Gaussian state [47]. (a) Bell factor S as a function of the squeezing λ. (b) Probability of success P_G of the generation of the non-Gaussian state as a function of the squeezing λ. The curves are plotted for perfect detectors ($\eta_{\rm PD} = \eta_{\rm BHD} = 100\%$) with $T = 0.9$ (solid line), $T = 0.95$ (dashed line), and $T = 0.99$ (dot-dashed line).

Figure 8(a) confirms that the Bell-CHSH inequality $|S| \leq 2$ can indeed be violated with the proposed set-up, and shows that there is an optimal squeezing $\lambda_{\rm opt}$ which maximizes S. This optimal squeezing is well predicted by the simplified model assuming ideal detectors with single-photon resolution, that is, $\lambda_{\rm opt}T \approx 0.57$. The maximum achievable Bell factor is $S_{\rm max} \approx 2.045$, which represents a violation of about 2.2%. To get close to $S_{\rm max}$, one needs sufficiently high (but not too strong) squeezing. In particular, the value $\lambda \approx 0.57$ corresponds to approximately 5.6 dB of squeezing. Figure 8(b) illustrates that there is a clear trade-off between S and the probability of success P_G. To maximize S, one should use highly transmitting beam splitters ($T \approx 1$), but this would drastically reduce P_G. The optimal T must be chosen depending on the details of the experimental implementation.

7.3. *Sensitivity to experimental imperfections*

Let us now study the sensitivity of this Bell test to the different imperfections that would necessarily occur in a realistic optical experiment, namely the non-unity efficiency and non-zero probability of false triggers of the photodetectors, the non-unity efficiency and noise of the homodyne detection, and the thermal noise in the two-mode squeezed vacuum state.

First, the Bell factor S depends only very weakly on the efficiency $\eta_{\rm PD}$ of the single-photon detectors, so the Bell-CHSH inequality can be violated even if $\eta_{\rm PD} \approx 1\%$. This is very important from the experimental point of view because, although the quantum detection efficiencies of the avalanche photodiodes may be of the order of 50%, the necessary spectral and spatial filtering which selects the mode that is detected by the photodetector may reduce the overall detection efficiency to a few percent. In practice, the minimum necessary $\eta_{\rm PD}$ will be determined mainly by the constraints on the total time of the experiment and by the dark counts of the detectors.

In contrast, the Bell factor S very strongly depends on the efficiency of the homodyne detectors, and $\eta_{\rm BHD}$ must be above $\approx 90\%$ in order to observe a Bell violation. However, this is not an obstacle because such (and even higher) homodyne efficiencies have already been achieved experimentally (see *e.g.* [48]). Interestingly, it was found in Ref. [47] that it is possible to partially compensate for the low homodyning efficiency by increasing the squeezing of the initial state.

The electronic noise of the homodyne detector is another factor that may reduce the observed Bell violation. As shown in Ref. [47], the electronic

noise should be $15-20$ dB below the shot noise, which is currently attainable with low-noise charge amplifiers. Again, higher squeezing can partially compensate for an increasing noise. Another source of noise originates from the state generation. In the analysis, it was assumed that the source emits a pure two-mode squeezed vacuum state. However, experimentally, it is very difficult to generate pure squeezed vacuum saturating the Heisenberg inequality. It is more realistic to consider a mixed Gaussian state. Here again, the added noise in the initial Gaussian state should be $15-20$ dB below the shot noise for a successful Bell test [47].

false triggers

Finally, a main source of imperfection that was observed in the experimental demonstration of single-photon subtraction in Ref. [46] comes from the false triggering of single-photon detectors. Indeed, a single-photon detector may be triggered by a photon coming from another mode than the one detected in the balanced homodyne detector. The single-mode description of a parametric amplifier is only an approximation, and the amplifier produces squeezed vacuum in several modes. A balanced homodyne detector very efficiently selects a single mode defined by the spatiotemporal profile of the local oscillator pulse. However, such a reference is missing in case of a single-photon detector, where the effective single mode has to be selected by spatial and spectral filtering, which reduces the overall detection efficiency $\eta_{\rm PD}$. In practice, this filtering is never perfect, hence the photodetector PD_A (PD_B) can sometimes click although no photon was removed from mode A (B). This false triggering can be modeled by re-defining the POVM element $\Pi_{1,C}$ (and $\Pi_{1,D}$) as a convex mixture of the original POVM element $I-|0\rangle\langle 0|$, which corresponds to a triggering by a photon coming from the mode A (B), and the identity operator I, which corresponds to a false triggering. As expected, the achievable Bell factor decreases with increasing probability of false triggers P_f. For a transmittance $T=0.95$, up to 6% of false triggers can be tolerated [47]. In the experiment reported in Ref. [46], the estimated fraction of false triggers was $P_f\approx 30\%$, which should thus be significantly reduced in order to realize a Bell test experiment. Possible ways of suppressing false triggers include better filtering and/or using sources that produce squeezed light in well defined spatial modes, such as nonlinear periodically poled waveguides.

8. Alternative schemes

It is interesting to analyze whether alternative schemes to the one studied so far may possibly lead to a larger violation of the Bell-CHSH inequalities,

therefore being more promising. Let us consider alternative schemes which involve from one to four photon subtractions. Since the probability of successful generation of a non-Gaussian state significantly decreases with the number of photon subtractions (while the complexity of the optical implementation increases with the number of photon subtractions), it is natural that the most interesting schemes for a Bell test are those involving only one photon subtraction. Unfortunately, none of the schemes with a single photon subtraction that were considered in Ref. [47] leads to a Bell violation, and it is unknown whether such a scheme can be found. The simplest schemes are then those involving two photon subtractions. In the preceding sections, it was shown that it is indeed possible to violate the Bell-CHSH inequality with the scheme of Fig. 4 involving two photon subtractions, giving $S_{\max,2\mathrm{ph}} = 2.048$. Several other schemes with two photon subtractions may also be devised which violate the Bell-CHSH inequality, but the achievable Bell factor S is smaller, see [47].

By adding one more photon subtraction, one can construct an ensemble of schemes with three photon subtractions. After numerical optimization, it was found in Ref. [47] that none of these schemes succeeds in violating the Bell-CHSH inequality. This striking result together with the fact that no interesting scheme based on a single photon subtraction has been found suggests that it may be necessary to subtract an even number of photons in order to observe $S > 2$.

Among the various schemes with four photon subtractions that were studied in Ref. [47], the most interesting one is obtained by applying two photon subtractions on each mode. Numerical calculations show that the maximum Bell violation is achieved for $T^2\lambda = 0.40$ and yields $S_{\max,4\mathrm{ph}} = 2.064$, which is indeed higher than the maximum achievable with two-photon subtraction, $S_{\max,2\mathrm{ph}} = 2.048$, and very close to the maximum value $S = 2.076$ obtained in Ref. [39]. Unfortunately, a more realistic description of the four-photon subtraction scheme that takes into account realistic imperfect detectors shows that, for $T < 0.95$, the fact that the photodetectors do not distinguish the number of photons reduces the Bell factor and dramatically decreases the probability of generating the non-Gaussian state ($P_G \approx 10^{-6}$). Therfore, it seems that, from a practical point of view, there is no advantage in using a scheme with four photon subtractions instead of the much simpler scheme with two photon subtractions shown in Fig. 4.

In a recent paper [49], another scheme has been proposed for generating a state of the form (3) reaching $S = 2.071$, which is very close to the maximum $S = 2.076$ of Ref. [39]. The state generation procedure needs

three successive photon subtractions interspersed by some Gaussification operation [31]. Unfortunately, a realistic description of the scheme that takes into account realistic imperfect detectors should necessarily bring the same conclusions as for the schemes with four photon subtractions.

9. Conclusions

In this Chapter, we have described an experimentally feasible setup allowing for a loophole-free Bell test with efficient homodyne detection. This scheme is based on a non-Gaussian entangled state which is conditionally generated from a two-mode squeezed vacuum state by subtracting a single photon from each mode. We have discussed the influence on the achievable Bell violation of the detector inefficiencies, the electronic noise of the homodyne detector, the impurity of the input state, and the effect of false triggers in the single-photon detectors. The main advantage of this scheme is that it is largely insensitive to the detection efficiency of the avalanche photodiodes that are used for the conditional preparation of the non-Gaussian state, so that efficiencies of the order of a few per cent are sufficient. We also have discussed several alternative schemes that involve the subtraction of one, two, three or four photons. The current conclusion is that there seems to be no advantage in using these other schemes instead of the above two-photon subtraction scheme.

This analysis makes it possible to define a set of realistic parameter values, which should be reached in a loophole-free Bell test : with $\eta = 30\%$, $T = 95\%$, and 6 dB of squeezing, a violation of the Bell-CHSH inequality by about 1% should be observable if the homodyne efficiency $\eta_{\rm BHD}$ is larger than 95% and less than 6% of false triggers impinge on the single-photon detectors. With a repetition rate of 1 MHz and $P \approx 2.6 \times 10^{-4}$, the number of data samples would be several hundreds per second, so that the required statistics to see a violation in the percent range could be obtained in a reasonable time (a few hours). In addition, the electronic noise of the homodyne detectors should be 15-20 dB below shot noise, which is attainable with low-noise charge amplifiers. All these numbers have already been reached separately in various experiments, but attaining them simultaneously certainly represents a serious challenge.

The very recent experimental demonstration of a single-photon subtraction from a single-mode squeezed vacuum state provides a strong incentive for further theoretical and experimental developments along these lines. In particular, the issues of more complex binnings, generalized Bell inequalities

in higher dimension, or multipartite Bell inequalities deserve further investigations. Any improvement of the amount of violation would certainly help making such a loophole-free Bell test possible with the present technology.

Acknowledgments

We would like to thank J. Eisert, Ph. Grangier, R. Tualle-Brouri, and J. Wenger for many stimulating discussions. We acknowledge financial support from the Communauté Française de Belgique under grant ARC 00/05-251, from the IUAP programme of the Belgian government under grant V-18, and from the EU under projects COVAQIAL (FP6-511004). R.G-P. acknowledges support from the Belgian foundation FRIA. JF also acknowledges support from the Project LN00A015 and Research Project No. CEZ: J14/98 of the Czech Ministry of Education.

References

1. A. Einstein, B. Podolsky, and N. Rosen, Phys. Rev. **47**, 777 (1935).
2. J. S. Bell, Physics (Long Island City, N.Y.) **1**, 195 (1964).
3. J. F. Clauser, M.A. Horne, A. Shimony and R.A. Holt, Phys. Rev. Lett. **23**, 880 (1969).
4. S. J. Freedman and J. F. Clauser, Phys. Rev. Lett. **28**, 938 (1972).
5. A. Aspect, P. Grangier, and G. Roger, Phys. Rev. Lett. **47**, 460 (1981).
6. A. Aspect, P. Grangier, and G. Roger, Phys. Rev. Lett. **49**, 91 (1982).
7. A. Aspect, J. Dalibard, and G. Roger, Phys. Rev. Lett. **49**, 1804 (1982).
8. P. G. Kwiat, K. Mattle, H. Weinfurter, A. Zeilinger, A. V. Sergienko, and Y. Shih, Phys. Rev. Lett. **75**, 4337 (1995).
9. G. Weihs, T. Jennewein, C. Simon, H. Weinfurter, and A. Zeilinger, Phys. Rev. Lett. **81**, 5039 (1998).
10. W. Tittel, J. Brendel, B. Gisin, T. Herzog, H. Zbinden, and N. Gisin, Phys. Rev. A **57**, 3229 (1998).
11. Philip M. Pearle, Phys. Rev. D **2**, 1418 (1970).
12. E. Santos, Phys. Rev. A **46**, 3646 (1992).
13. P. G. Kwiat, P. H. Eberhard, A. M. Steinberg, and R. Y. Chiao, Phys. Rev. A **49**, 3209 (1994).
14. M.A. Rowe, D. Kielpinski, V. Meyer, C.A. Sackett, W. M. Itano, C. Monroe, and D.J. Wineland, Nature (London) **409**, 791 (2001).
15. J.S. Bell, Speakable and Unspeakable in Quantum Mechanics (Cambridge University Press, Cambridge, 1988).
16. E. Santos, Phys. Lett. A **200**, 1 (1995).
17. C. Simon and W.T.M. Irvine, Phys. Rev. Lett. **91**, 110405 (2003).
18. X.-L. Feng, Z.-M. Zhang, X.-D. Li, S.-Q. Gong, and Z.-Z. Xu, Phys. Rev. Lett. **90**, 217902 (2003).
19. L. M. Duan and H. J. Kimble, Phys. Rev. Lett. **90**, 253601 (2003).

20. D. E. Browne, M. B. Plenio, and S. F. Huelga, Phys. Rev. Lett. **91**, 067901 (2003)
21. B. B. Blinov, D. L. Moehring, L. M. Duan, and C. Monroe, Nature (London) **428**, 153 (2004).
22. E. S. Fry, T. Walther, and S. Li, Phys. Rev. A **52**, 4381 (1995).
23. M. Freyberger, P. K. Aravind, M. A. Horne, and A. Shimony, Phys. Rev. A **53**, 1232 (1996).
24. E. S. Polzik, J. Carri, and H. J. Kimble, Phys. Rev. Lett. **68**, 3020 (1992).
25. Z. Y. Ou, S. F. Pereira, H. J. Kimble, and K. C. Peng, Phys. Rev. Lett. **68**, 3663-3666 (1992).
26. C. Schori, J. L. Sørensen, and E. S. Polzik, Phys. Rev. A **66**, 033802 (2002).
27. W. P. Bowen, R. Schnabel, P. K. Lam, and T. C. Ralph, Phys. Rev. A **69**, 012304 (2004).
28. J. Eisert, S. Scheel, and M.B. Plenio, Phys. Rev. Lett. **89**, 137903 (2002).
29. J. Fiurášek, Phys. Rev. Lett. **89**, 137904 (2002).
30. G. Giedke and J.I. Cirac, Phys. Rev. A **66**, 032316 (2002).
31. D. E. Browne, J. Eisert, S. Scheel, and M. B. Plenio, Phys. Rev. A **67**, 062320 (2003).
32. J. Eisert, D. Browne, S. Scheel, and M. B. Plenio, Annals of Physics (NY) **311**, 431 (2004).
33. K. Banaszek and K. Wódkiewicz, Phys. Rev. A **58**, 4345 (1998).
34. Z.-B. Chen, J.-W. Pan, G. Hou, and Y.-D. Zhang, Phys. Rev. Lett. **88**, 040406 (2002).
35. L. Mišta, Jr., R. Filip, and J. Fiurášek, Phys. Rev. A **65**, 062315 (2002).
36. R. Filip and L. Mišta, Jr., Phys. Rev. A **66**, 044309 (2002).
37. A. Gilchrist, P. Deuar, and M. D. Reid, Phys. Rev. Lett. **80**, 3169 (1998).
38. A. Gilchrist, P. Deuar, and M. D. Reid, Phys. Rev. A **60**, 4259 (1999).
39. W. J. Munro, Phys. Rev. A **59**, 4197 (1999).
40. J. Wenger, M. Hafezi, F. Grosshans, R. Tualle-Brouri, and P. Grangier, Phys. Rev. A **67**, 012105 (2003).
41. R. García-Patrón, J. Fiurášek, N. J. Cerf, J. Wenger, R. Tualle-Brouri, and Ph. Grangier, Phys. Rev. Lett. **93**, 130409 (2004).
42. H. Nha and H. J. Carmichael, Phys. Rev. Lett. **93**, 020401 (2004).
43. T. Opatrný, G. Kurizki, and D.-G. Welsch, Phys. Rev. A **61**, 032302 (2000).
44. P. T. Cochrane, T. C. Ralph, and G. J. Milburn, Phys. Rev. A **65**, 062306 (2002).
45. S. Olivares, M. G. A. Paris, and R. Bonifacio, Phys. Rev. A **67**, 032314 (2003).
46. J. Wenger, R. Tualle-Brouri, and Ph. Grangier, Phys. Rev. Lett. **92**, 153601 (2004).
47. R. García-Patrón, J. Fiurášek, N. J. Cerf, Phys. Rev. A **71**, 022105 (2005).
48. T. C. Zhang, K. W. Goh, C. W. Chou, P. Lodahl, and H. J. Kimble, Phys. Rev. A **67**, 033802 (2003).
49. S. Daffer and P. L. Knight, Phys. Rev. A **72**, 032509 (2005).